Inhibition of p38α MAPK rescues cardiomyopathy induced by overexpressed β_2-adrenergic receptor, but not β_1-adrenergic receptor

Pallavi S. Peter,[1] Jennifer E. Brady,[1] Lin Yan,[1] Wei Chen,[1] Stefan Engelhardt,[2] Yibin Wang,[3] Junichi Sadoshima,[1] Stephen F. Vatner,[1] and Dorothy E. Vatner[1]

[1]Department of Cell Biology and Molecular Medicine, Cardiovascular Research Institute, New Jersey Medical School, University of Medicine and Dentistry of New Jersey, Newark, New Jersey, USA. [2]Rudolf Virchow Center, Deutsche Forschungsgemeinschaft Research Center for Experimental Biomedicine, University of Wuerzburg, Wuerzburg, Germany. [3]Department of Anesthesiology and Medicine, Molecular Biology Institute, David Geffen School of Medicine, UCLA, Los Angeles, California, USA.

We examined the role of p38α MAPK in mediating cardiomyopathy in mice overexpressing β_1-adrenergic receptor (β_1-AR) or β_2-AR by mating them with dominant-negative p38α (DNp38α) MAPK mice. Both β_1-AR and β_2-AR Tg mice had enhanced LV ejection fraction (LVEF) as young adults and developed similar cardiomyopathy at 11–15 months, characterized by reduced LVEF, myocyte hypertrophy, fibrosis, and apoptosis. We inhibited p38α MAPK by mating β_1-AR Tg and β_2-AR Tg mice with DNp38α MAPK mice, which rescued the depressed LVEF and reduced apoptosis and fibrosis in bigenic β_2-AR × DNp38α MAPK mice, but not bigenic β_1-AR × DNp38α MAPK mice, and failed to reduce myocyte hypertrophy in either group. $G_{s\alpha}$ was increased in both β_1-AR Tg and β_2-AR Tg mice and was still present in bigenic β_1-AR × DNp38α MAPK mice, but not bigenic β_2-AR × DNp38α MAPK mice. This suggests that p38α MAPK is one critical downstream signal for the development of cardiomyopathy following chronic β_2-AR stimulation, but other kinases may be more important in ameliorating the adverse effects of chronic β_1-AR stimulation.

Introduction

Chronic β-adrenergic receptor (β-AR) stimulation is deleterious and is involved in the pathogenesis of heart failure (HF) (1–8). There are several Tg mouse models where β-AR signaling is chronically enhanced by overexpression of cardiac β_1-AR (3), β_2-AR (2, 6, 7), or $G_{s\alpha}$ (5, 8). These Tg mice develop cardiomyopathy as they age, as reflected by reduced LV function, enhanced fibrosis, apoptosis, and myocyte hypertrophy. Clinical data supporting this concept include the deterioration and enhanced mortality of patients in HF receiving sympathomimetics (4); conversely, there is now convincing evidence of reduced morbidity and mortality of patients in HF on chronic β-AR blockade therapy (1). Whereas chronic β-AR blockade therapy is assuming increasing importance in HF, the cellular and/or molecular mechanisms mediating this beneficial action are less well understood. One mechanism mediating the beneficial effects of β-AR blockade therapy involves reversing PKA hyperphosphorylation of the calcium release channel/cardiac ryanodine receptor (9, 10).

We also reasoned that in view of the resemblance between the deleterious effects of chronic sympathomimetic amine therapy in patients with HF and the development of cardiomyopathy in mouse models overexpressing components of the β-AR signaling pathway, identifying the molecular mechanisms responsible for reversing the cardiomyopathy in these mouse models of chronically enhanced β-AR signaling might also shed light on potential mechanisms involved in β-AR blockade therapy in HF. Several members of the MAPK superfamily — which consists of ERKs and 2 stress-responsive subfamilies, JNKs and p38 MAPK kinases — are important mediators of cell growth and stress stimuli (11), and in the mammalian heart these kinases regulate myocyte growth in response to pathologic stimuli. Importantly, in mice with overexpressed cardiac $G_{s\alpha}$, the activity of several of these stress-activated kinases is enhanced in the heart as the mice develop cardiomyopathy; moreover, their activity is reduced following chronic β-AR blockade (12).

To examine the consequences of chronic β_1-AR and β_2-AR activation, we examined the cardiac phenotype of old mice (11–15 months) with β_1-AR and β_2-AR overexpression. Our initial results in the present study suggested that not only β_1-AR overexpression, but also β_2-AR overexpression, induced cardiomyopathy in adult animals. In vitro studies have suggested differential activation of p38α MAPK by β_1-AR and β_2-AR (13) and that β_1-AR and β_2-AR affect apoptosis and myocyte hypertrophy differently, that is, it has been proposed that activation of β_2-AR significantly protects the myocardium from apoptosis (14–17) and hypertrophy (18, 19). Thus, we sought to examine the role of p38α MAPK in mediating cardiomyopathy in mice with β_1-AR and β_2-AR overexpression. If the p38α MAPK molecule was responsible for the cardiomyopathy, then mating the Tg mice with dominant-negative p38α (DNp38α) MAPK mice (13, 20) should ameliorate the cardiomyopathy. Accordingly, we examined the development of cardiomyopathy in β_1-AR Tg and β_2-AR Tg mice, and whether mating these mice with DNp38α MAPK Tg mice would result in a lineage of bigenic mice that would be rescued from cardiomyopathy. We found that

Nonstandard abbreviations used: AR, adrenergic receptor; DN, dominant-negative; HF, heart failure; LVEF, LV ejection fraction; Mst-1, mammalian sterile 20-like kinase 1; p-, phosphorylated; TL, tibial length.

Conflict of interest: The authors have declared that no conflict of interest exists.

Citation for this article: *J. Clin. Invest.* **117**:1335–1343 (2007). doi:10.1172/JCI29576.

Table 1
Echocardiographic results

	WT	DNp38α	β1-AR Tg	Bigenic β1-AR Tg × DNp38α MAPK	β2-AR Tg	Bigenic β2-AR Tg × DNp38α MAPK
Young						
n	7	3	6	3	6	3
LVEF (%)	71 ± 1	72 ± 3	81 ± 2[A]	71 ± 4	84 ± 2[A]	84 ± 1[A]
Fractional shortening (%)	34 ± 0.8	34 ± 2.4	43 ± 1.8[A]	34 ± 3	46 ± 2.7[A]	46 ± 1.2[A]
Heart rate (bpm)	423 ± 20	467 ± 20	507 ± 18	449 ± 33	551 ± 51[A]	651 ± 4[A]
End-diastolic diameter (mm)	3.7 ± 0.1	3.7 ± 0.1	3.4 ± 0.1	3.3 ± 0.1	3.2 ± 0.1[A]	3.3 ± 0.2
End-systolic diameter (mm)	2.4 ± 0.1	2.4 ± 0.1	1.9 ± 0.1[A]	2.1 ± 0.1	1.7 ± 0.1[A]	1.8 ± 0.1[A]
Old						
n	9	10	9	7	9	10
LVEF (%)	70 ± 1	76 ± 2	47 ± 3[A,B]	54 ± 2[A]	47 ± 4[A,B]	79 ± 2[A,C]
Fractional shortening (%)	33 ± 1.0	38 ± 1.6[A]	20 ± 1.7[A,B]	23 ± 1.1[A]	20 ± 2[A,B]	41 ± 2.2[A,C]
Heart rate (bpm)	437 ± 16	444 ± 21	510 ± 19[A]	565 ± 21[A]	582 ± 23[A]	603 ± 16[A]
End-diastolic diameter (mm)	3.9 ± 0.1	4.0 ± 0.1	4.6 ± 0.1[A,B]	4.7 ± 0.2[A,B]	4.5 ± 0.3[A,B]	3.8 ± 0.2[C]
End-systolic diameter (mm)	2.6 ± 0.1	2.5 ± 0.1	3.7 ± 0.2[A,B]	3.6 ± 0.2[A,B]	3.7 ± 0.3[A,B]	2.2 ± 0.1

[A]$P < 0.05$ versus WT of the same age. [B]$P < 0.05$ versus young mice of the same group. [C]$P < 0.05$ versus old Tg.

inhibition of p38α MAPK in bigenic mice rescued the depressed LV ejection fraction (LVEF) and reduced apoptosis and fibrosis in β_2-AR Tg mice but not β_1-AR Tg mice, and myocyte hypertrophy was not reduced in either bigenic model. This suggests that p38α MAPK is one critical downstream signal for the development of cardiomyopathy following chronic β_2-AR stimulation, but other kinases may be more important in ameliorating the adverse effects of chronic β_1-AR stimulation.

Results

LV function. LVEF was higher in young (4–6 months) β_1-AR Tg mice (81% ± 2%) and β_2-AR Tg mice (84% ± 2%) than in young WT mice (71% ± 1%; $P < 0.01$) and in young DNp38α MAPK mice (72% ± 3%; $P < 0.01$). The heart rates of β_1-AR Tg and β_2-AR Tg mice were also higher than that of WT mice (Table 1).

Both β_1-AR Tg and β_2-AR Tg mice developed cardiomyopathy by 11–15 months of age, as evidenced by their lower LVEF (β_1-AR, 47% ± 3%; β_2-AR, 47% ± 4%), fractional shortening, and dilated LV cavity during diastole and systole (Table 1). Interestingly, old bigenic β_2-AR Tg × DNp38α MAPK mice maintained normal cardiac function and normal LV cavity size compared with age-matched WT mice (Figure 1). Furthermore, they exhibited normal LV functional reserve, as reflected by increased LVEF in response to ISO (0.04 μg/kg/min) from 68% ± 1% to 79% ± 2%, similar to that of old WT mice, which demonstrated an LVEF increase in response to ISO from 70% ± 3% to 78% ± 2%. However, old bigenic β_1-AR Tg × DNp38α MAPK mice demonstrated no rescue of LV function, as LVEF remained depressed (54% ± 2%) and LV end-diastolic cavity size remained dilated.

LV pathology. In all groups of young mice, there was no difference in the LV mass as assessed by the ratios of LV wt/tibial length (LV wt/TL) and LV/body wt compared with WT mice, but old β_1-AR and β_2-AR Tg mice had higher LV wt/TL and LV/body wt ratios than did age-matched WT mice (Table 2). LV/body wt and LV wt/TL ratios, indices of LV hypertrophy, were not rescued in bigenic β_1-AR Tg × DNp38α MAPK mice, but were diminished modestly in bigenic β_2-AR Tg × DNp38α MAPK mice. The lung wt/TL ratio, an index of LV decompensation, was also elevated in old β_1-AR Tg and remained elevated in old bigenic β_1-AR Tg × DNp38α MAPK mice. In contrast, while lung wt/TL was also increased in old β_2-AR Tg mice, it was not significantly elevated in old bigenic β_2-AR Tg × DNp38α MAPK mice.

Histology. Staining with H&E revealed abnormal histological architecture (i.e., increased necrosis and interstitial fibrosis) in old β_1-AR Tg and β_2-AR Tg mice (Figure 2). Old β_1-AR Tg mice had a 12-fold increase in fibrosis compared with old WT mice, as quantified by picric acid sirius red staining (6.9% ± 1.3% versus 0.6% ± 0.04%; $P < 0.01$), and a similar increase in fibrosis was observed in the old bigenic β_1-AR Tg × DNp38α MAPK mice (5.9% ± 1.1%; Figure 3A). Old β_2-AR Tg mice also exhibited an increase in fibrosis (5.2% ± 0.4%). However, fibrosis was significantly diminished ($P < 0.05$) in bigenic β_2-AR Tg × DNp38α MAPK mice compared with β_2-AR Tg mice (3.5% ± 0.5%; Figure 2H and Figure 3A).

Apoptosis, as quantitated by TUNEL, increased 17-fold in old β_1-AR Tg mice (3.1% ± 0.9%; $P < 0.05$) and to a similar extent in old bigenic β_1-AR Tg × DNp38α MAPK mice (2.8% ± 0.6%; $P < 0.05$) compared with age-matched WT mice (0.2% ± 0.08%; Figure 3B). Apoptosis also increased in β_2-AR Tg mice (3.8% ± 0.6%), but was reduced in bigenic β_2-AR Tg × DNp38α MAPK mice (1.8% ± 0.3%; $P < 0.05$).

Myocyte cross-sectional area, quantitated by wheat germ agglutinin, increased 2-fold in old β_1-AR Tg mouse hearts (380 ± 3.4 μm^2; $P < 0.01$) and was not diminished in hearts of bigenic β_1-AR Tg × DNp38α MAPK mice compared with those of WT mice (372 ± 7.9 μm^2 versus 209 ± 1 μm^2; Figure 3C). Myocyte cross-sectional area also increased in the hearts of β_2-AR Tg mice (311 ± 29 μm^2; $P < 0.01$) and was not diminished in bigenic β_2-AR Tg × DNp38α MAPK mice compared with WT mice (308 ± 24 μm^2 versus 193 ± 13 μm^2; Figure 2I and Figure 3C). Old DNp38α MAPK mice exhibited a moderate increase in myocyte cross-sectional area (232 ± 7 μm^2), consistent with the increased LV/body wt ratio shown in Table 2, which was not large enough to account for the failure of the old bigenic mice to show decreased LV myocyte cross-sectional area.

Western blotting. The level of total p38 MAPK was significantly higher in both bigenic groups (Figure 4A). Both old β_1-AR and old β_2-AR Tg mice had higher levels of phosphorylated p38 (p-p38) MAPK compared with age-matched WT mice (Figure 4B). However,

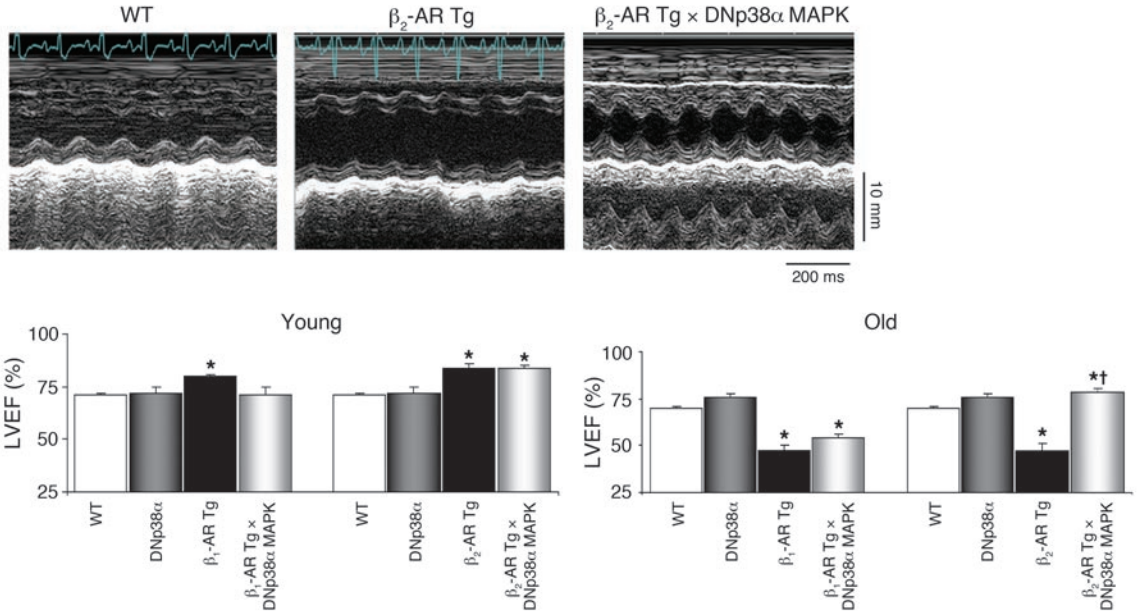

Figure 1
Echocardiographic measurements of LVEF. Top panels show representative LV M-mode echocardiographic recordings of old WT, old β_2-AR Tg, and old bigenic β_2-AR Tg × DNp38α MAPK mice, showing the dilated, poorly contracting heart in old β_2-AR Tg mice that was rescued in the bigenic β_2-AR Tg × DNp38α MAPK mice. Graphs show mean ± SEM data for LVEF for WT, DNp38α, β_1-AR Tg, β_1-AR Tg × DNp38α MAPK, β_2-AR Tg, and bigenic β_2-AR Tg × DNp38α MAPK mice. The number of mice per group is shown in Table 1. LVEF was significantly increased in young β_1-AR Tg and β_2-AR Tg mice and significantly depressed in old β_1-AR Tg and β_2-AR Tg mice compared with age-matched WT mice. LVEF remained depressed in old bigenic β_1-AR Tg × DNp38α MAPK mice, but in contrast, old bigenic β_2-AR Tg × DNp38α MAPK mice exhibited rescued LV function. *P < 0.05 versus WT; †P < 0.05 versus corresponding Tg.

p-p38 MAPK was not elevated in either bigenic group compared with WT mice. Furthermore, we examined the downstream molecule of p38, MAPKAPK2, and found the level of total MAPKAPK2 was significantly higher in both bigenic groups (Figure 4C), but the level of p-MAPKAPK2 (Thr^{222}) was significantly lower in both bigenic groups (Figure 4D), suggesting that p38 MAPK is inactivated. There were no differences in the levels of p-ERK and p-JNK in any of the experimental groups (Figure 5). Both old β_1-AR and old β_2-AR Tg mice demonstrated increases in $G_{s\alpha}$ (Figure 6) and decreases in $G_{i\alpha}$ (Figure 7). The increases in $G_{s\alpha}$ were not sustained

Table 2
Pathology

	WT	DNp38α	β1-AR Tg	Bigenic β1-AR Tg × DNp38α MAPK	β2-AR Tg	Bigenic β2-AR Tg × DNp38α MAPK
Young						
n	7	3	5	3	6	3
LV wt (mg)	84 ± 5	91 ± 9	77 ± 3	71 ± 7	75 ± 4	81 ± 2
Lung wt (mg)	170 ± 4	166 ± 1	169 ± 5	161 ± 13	155 ± 7	169 ± 12
Body wt (g)	30 ± 1.6	27 ± 2.9	31 ± 1.1	26 ± 2.0	25 ± 1.8	26 ± 2.6
LV wt/TL	4.7 ± 0.3	5.0 ± 0.4	4.3 ± 0.2	4.0 ± 0.4	4.2 ± 0.2	4.6 ± 0.1
LV/body wt	2.8 ± 0.1	33 ± 0.1	2.5 ± 0.1	2.7 ± 0.1	3.0 ± 0.1	3.1 ± 0.2
Lung wt/TL	9.5 ± 0.2	9.1 ± 0.1	9.5 ± 0.3	9.1 ± 0.7	8.7 ± 0.4	9.5 ± 0.5
Old						
n	9	10	9	7	9	10
LV wt (mg)	93 ± 3	127 ± 9[A,B]	118 ± 3[A,B]	139 ± 10[A,C]	129 ± 7[A,B]	116 ± 6[A]
Lung wt (mg)	181 ± 5	198 ± 11	281 ± 40[A,B]	288 ± 53[A]	289 ± 39[A,B]	196 ± 8[C]
Body wt (g)	34 ± 1.4	39 ± 2.3[A,B]	30 ± 1.9	31 ± 3.0	34 ± 2.2[B]	35 ± 2.4
LV wt/TL	5.1 ± 0.2	6.9 ± 0.5[A,B]	6.5 ± 0.2[A,B]	7.7 ± 0.5[A]	6.9 ± 0.4[A,B]	6.2 ± 0.3[A]
LV/body wt	2.8 ± 0.2	3.2 ± 0.1	4.2 ± 0.4[A,B]	4.7 ± 0.6[A,B]	3.9 ± 0.3[A,B]	3.3 ± 0.1
Lung wt/TL	9.9 ± 0.2	10.8 ± 0.6	15.6 ± 2.2[A,B]	15.8 ± 2.8[A]	15.4 ± 2.1[A,B]	10.5 ± 0.5[C]

[A]P < 0.05 versus WT of the same age. [B]P < 0.05 versus young mice of the same group. [C]P < 0.05 versus old Tg.

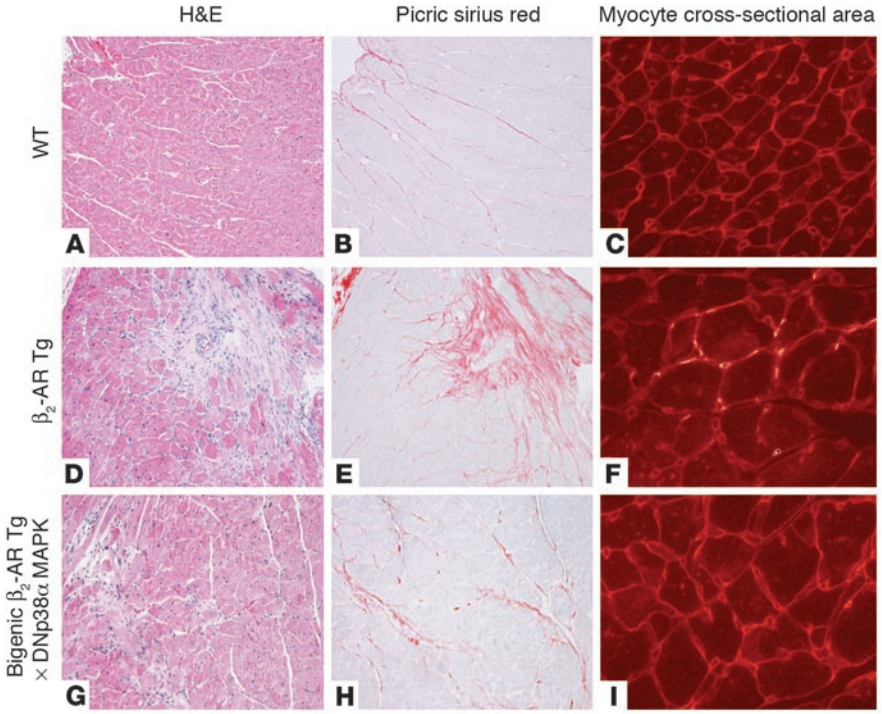

Figure 2
Histological examples of the necrosis and fibrosis in old WT (**A**–**C**), old β_2-AR Tg (**D**–**F**), and old bigenic β_2-AR Tg × DNp38α MAPK mice (**G**–**I**) are shown in H&E stains (**A**, **D**, and **G**; original magnification, ×4). Picric acid sirius red staining (**B**, **E**, and **H**; original magnification, ×10) was used to quantitate collagen. Myocyte cross-sectional area was visualized using wheat germ agglutinin staining (**C**, **F**, and **I**; original magnification, ×40). The enlarged myocytes for both β_2-AR Tg and bigenic β_2-AR Tg × DNp38α MAPK mice. Note that there were marked increases in fibrosis and necrosis in β_2-AR Tg mice, which were ameliorated substantially in bigenic β_2-AR Tg × DNp38α MAPK mice.

in old bigenic β_2-AR Tg × DNp38α MAPK mice, but were still present in old bigenic β_1-AR Tg × DNp38α MAPK mice (Figure 6).

We have previously shown that mammalian sterile 20-like kinase 1 (Mst-1) is activated by stresses in the heart, including ischemia/reperfusion and pressure overload, which in turn plays an important role in mediating myocyte apoptosis and progression of congestive HF in mice (21). Mst-1 is activated by caspase-3–dependent cleavage, and thus the appearance of 34- to 36-kDa forms of Mst-1 coincides with the occurrence of apoptosis (21). Immunoblot analyses of myocardial homogenates showed that the caspase-3–cleaved form of Mst-1 was clearly present in β_1-AR Tg mice, but not β_2-AR Tg mice, and that expression of DNp38α MAPK failed to abolish the

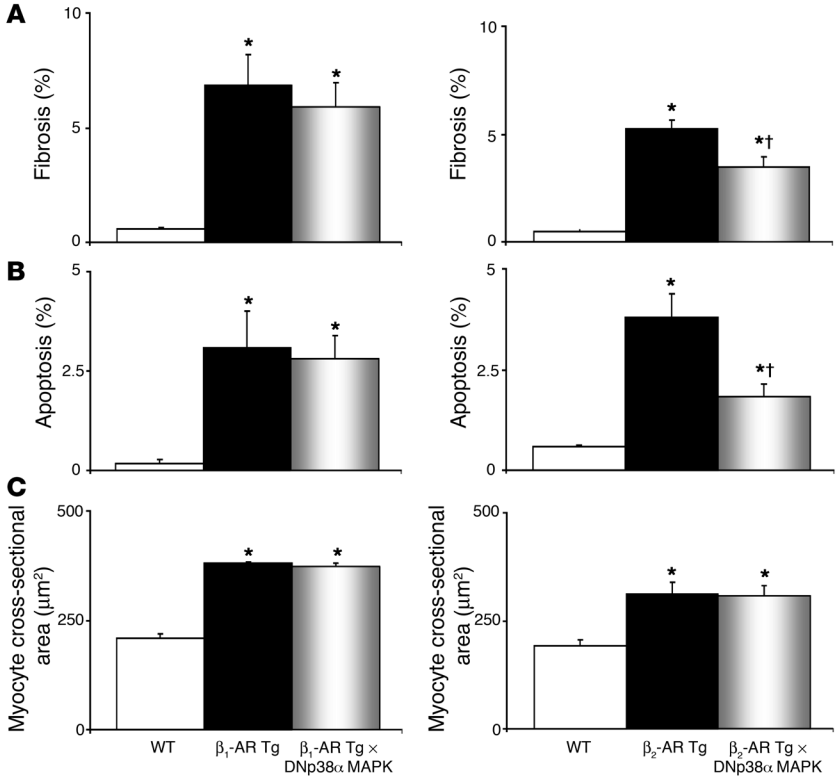

Figure 3
Fibrosis, apoptosis, and myocyte cross-sectional area in old WT, β_1-AR Tg, bigenic β_1-AR Tg × DNp38α MAPK, β_2-AR Tg, and bigenic β_2-AR Tg × DNp38α MAPK mice. (**A**) Fibrosis, as assessed by quantitating collagen with picric acid sirius red staining, was significantly increased in both β_1-AR Tg and β_2-AR Tg mice compared with WT mice. Fibrosis was significantly reduced in bigenic β_2-AR Tg × DNp38α MAPK mice, but not bigenic β_1-AR Tg × DNp38α MAPK mice, compared with β_2-AR Tg and β_1-AR Tg mice, respectively. (**B**) Apoptosis, as assessed by TUNEL, was significantly increased in both β_1-AR Tg and β_2-AR Tg mice compared with WT mice. Apoptosis was significantly reduced in bigenic β_2-AR Tg × DNp38α MAPK mice, but not bigenic β_1-AR Tg × DNp38α MAPK mice, compared with β_2-AR Tg and β_1-AR Tg mice, respectively. (**C**) The myocyte cross-sectional area was significantly increased in both β_1-AR Tg and β_2-AR Tg mice. There was no reduction in myocyte cross-sectional area in either bigenic β_1-AR Tg × DNp38α MAPK mice or bigenic β_2-AR Tg × DNp38α MAPK mice compared with β_1-AR Tg and β_2-AR Tg mice, respectively. Data are mean ± SEM. $^*P < 0.05$ versus WT; $^\dagger P < 0.05$ versus corresponding Tg.

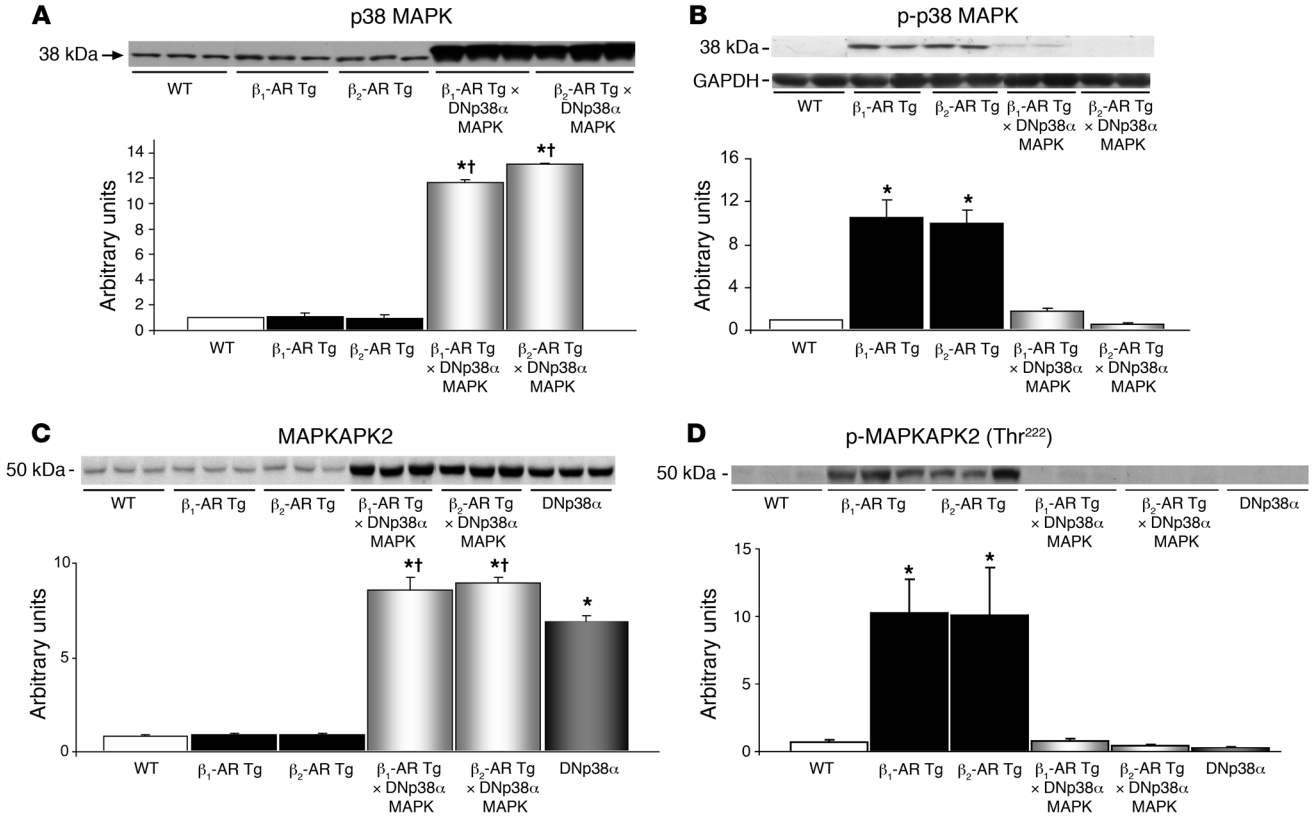

Figure 4

p38 and MAPKAPK2. (**A**) Total p38 MAPK levels were significantly higher due to transgene expression in both old bigenic β_1-AR Tg × DNp38α MAPK and old β_2-AR Tg × DNp38α MAPK mice compared with old β_1-AR Tg and old β_2-AR Tg mice, respectively, as well as with old WT mice. (**B**) Levels of p-p38 MAPK increased significantly in old β_1-AR Tg and old β_2-AR Tg mice compared with age-matched WT mice and were not increased in bigenic mice. (**C**) Total MAPKAPK2 levels were significantly higher in old bigenic β_1-AR Tg × DNp38α MAPK, old bigenic β_2-AR Tg × DNp38α MAPK mice, and DNp38α mice compared with age-matched WT mice. Both bigenic groups had levels significantly higher than those of their corresponding Tg groups. (**D**) Levels of p-MAPKAPK2 increased significantly in old β_1-AR Tg and old β_2-AR Tg mice compared with age-matched WT mice and were not increased in old bigenic mice. DNp38α mice were used as controls. $n = 4$ mice per group, with the exception of β_1-AR Tg mice in **C** and **D** ($n = 5$). *$P < 0.05$ versus WT; †$P < 0.05$ versus corresponding Tg.

presence of the caspase-3–cleaved form of Mst-1 in β_1-AR Tg mice (Figure 8). These results suggest that the proapoptotic signaling mechanism remains active in bigenic β_1-AR Tg × DNp38α MAPK mice and that the residual activity of Mst-1 may play an important role in mediating the cardiomyopathy in bigenic β_1-AR Tg × DNp38α MAPK mice. We also examined the levels of Akt and p-Akt in these mice. The level of p-Akt was significantly higher in β_1-AR Tg mice than in WT mice, which could be another mechanism involved in the regulation of cardiomyopathy in β_1 mice (Figure 9).

Discussion

It is well recognized that stimulation of the β-AR signaling pathways activates a variety of stress-activated kinases, such as p38 MAPK, JNKs, and ERK1/2 (22, 23). In the overexpressed $G_{s\alpha}$ model, the transition from hyperfunction to cardiomyopathy coincides with activation of p38 MAPK (12); this is also observed with the development of $G_{\alpha q}$ cardiomyopathy (24). It is also well recognized that β-AR stimulation induces myocyte hypertrophy and apoptosis, which can also be mediated by p38α MAPK in vitro (25), and that p38α MAPK induces hypertrophy and apoptosis, critical features of cardiomyopathy (25–27). Accordingly, we examined the extent to which this pathway was involved in mediating cardiomyopathy caused by cardiac overexpression of either β_1-AR or β_2-AR. The most striking finding of this investigation was that the cardiomyopathy in mice with β_2-AR overexpression, but not β_1-AR overexpression, was markedly attenuated by inhibition of p38α MAPK in bigenic mice harboring the *DNp38α MAPK* gene. Even though there were differences in the number of copies of β_1-AR and β_2-AR genes, for the purpose of this comparison it is critical to note that p38α MAPK activity increased to a similar extent as cardiomyopathy developed, and both models behaved similarly in vivo: both demonstrated enhanced LV function as young adults and developed equivalent levels of cardiomyopathy at the same ages (11–15 months). Furthermore, both WT groups behaved identically. In addition, in young adults, baseline and stimulated adenylyl cyclase activity were similar in both models. The data on adenylyl cyclase activity were not included because they confirm what has been published previously (6). Importantly, the decreased LVEF (47% ± 3% and 47% ± 4% versus 70% ± 1% in WT) and increased collagen (6.9% ± 1.3% and 5.2% ± 0.4% versus 0.6% ± 0.04% in WT), apoptosis (3.1% ± 0.9% and 3.8% ± 0.6 % versus 0.2% ± 0.08% in WT), and LV hypertrophy (i.e., LV wt/TL, 6.5% ± 0.2% and 6.9% ± 0.4% versus 5.1% ± 0.2% in WT) were almost identical in β_1-AR Tg and β_2-AR Tg mice. However, the bigenic β_1-AR Tg × DNp38α MAPK mice did not exhibit ameliora-

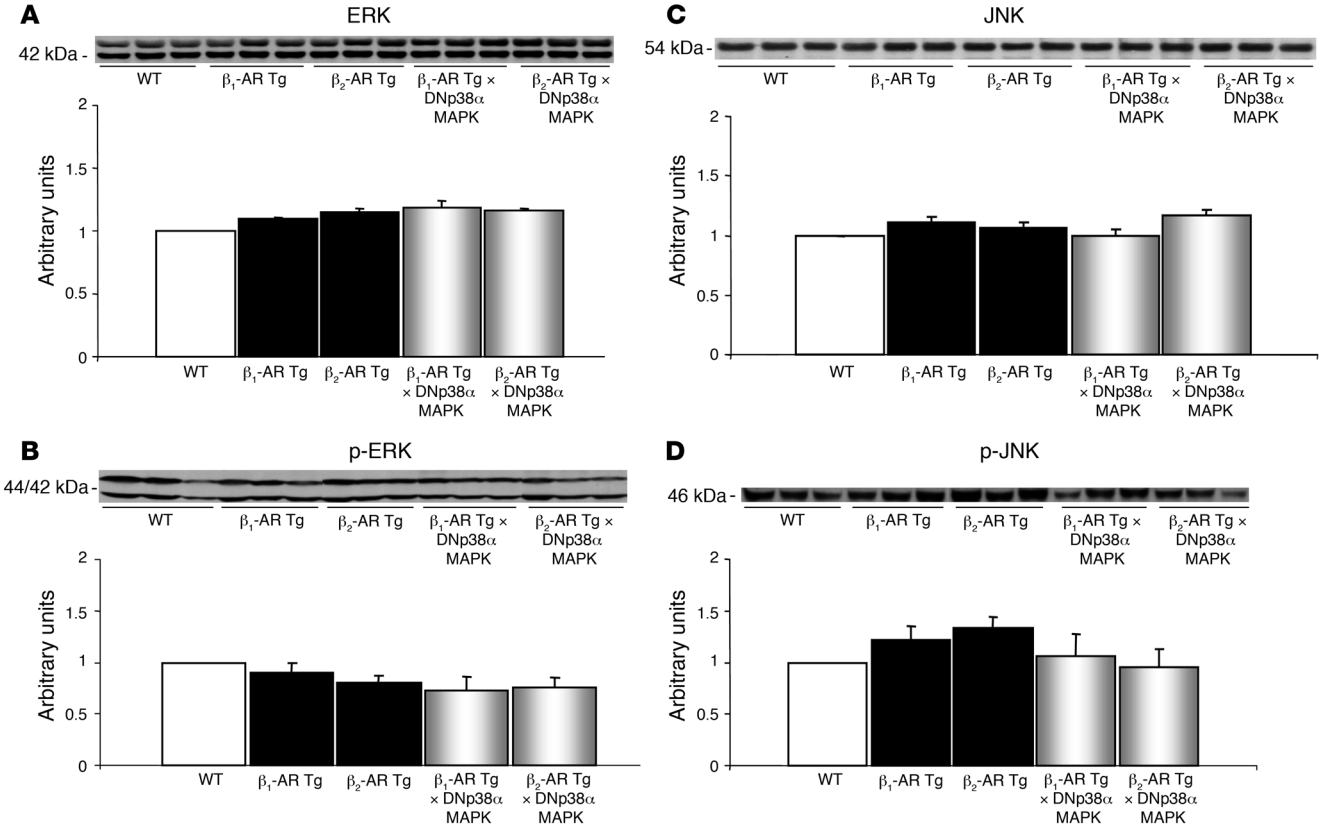

Figure 5
ERK and JNK. There were no significant differences in the levels of ERK (**A**), p-ERK (**B**), JNK (**C**), and p-JNK (**D**) in any of the experimental groups. $n = 4$ mice per group.

tion of any aspects of cardiomyopathy, whereas with β_2-AR overexpression, the bigenic β_2-AR × DNp38α MAPK mice were markedly protected from the development of cardiomyopathy.

Although the depressed LV function in old β_2-AR Tg mice was completely rescued in the bigenic β_2-AR Tg × DNp38α MAPK mouse model, the extent of apoptosis and fibrosis was reduced ($P < 0.05$), but not eliminated. This could be because of the residual p38α MAPK activity in the bigenic mice, or it could implicate other stress-activated MAPKs in mediating cardiomyopathy. In support of the latter explanation, in both bigenic groups, the p38α MAPK activity levels (Figure 4B) as well as the downstream MAPKAPK2 activity of p38α MAPK (Figure 4C) were effectively diminished, as assessed by Western blotting. Therefore, the residual development of apoptosis and fibrosis in the bigenic mice most likely arose from a different MAPK pathway. This is also the most likely explanation as to why the bigenic β_1-AR Tg × DNp38α MAPK mice did not show improvement, that is, other MAPKs are likely involved. In support of this, expression of DNp38α MAPK failed to abolish the presence of the caspase-3–cleaved form of Mst-1 in β_1-AR Tg mice (Figure 8). Other MAPKs, such as Mst-1, may be responsible for the persistent apoptosis and cardiomyopathy in the bigenic β_1-AR Tg × DNp38α MAPK mice. In addition, p-Akt was elevated only in β_1-AR Tg and bigenic β_1-AR Tg × DNp38α MAPK mice. The β_1-AR–stimulated apoptosis could involve the mitochondrial pathway, since cytochrome *c* release into the cytosol was observed (data not shown). Another potential explanation could be related to the increased $G_{s\alpha}$, which was not observed in the bigenic β_2-AR Tg × DNp38α MAPK mice but present in the bigenic β_1-AR Tg ×

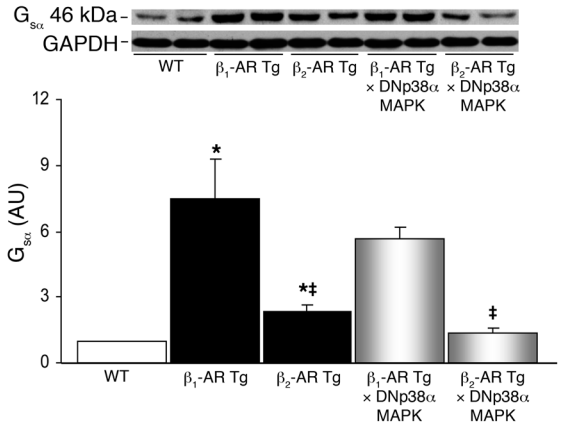

Figure 6
$G_{s\alpha}$ was increased in LVs of both old β_1-AR Tg and old β_2-AR Tg mice compared with age-matched WT mice, but the increase was greater in β_1-AR Tg mice than in β_2-AR Tg mice. Furthermore, old bigenic β_2-AR Tg × DNp38α MAPK mice no longer demonstrated an increase in $G_{s\alpha}$, whereas increased $G_{s\alpha}$ persisted in old bigenic β_1-AR Tg × DNp38α MAPK mice. *$P < 0.05$ versus WT; ‡$P < 0.05$ versus β_1-AR Tg.

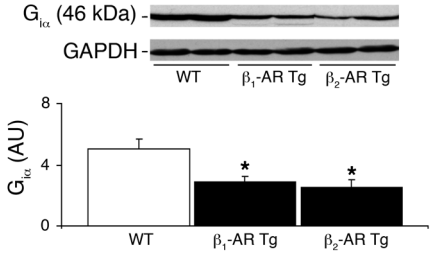

Figure 7
$G_{i\alpha}$ was decreased in both old β_1-AR Tg and old β_2-AR Tg mice compared with age-matched WT mice. *$P < 0.05$ versus WT.

DNp38α MAPK mice. It has also been shown by Zheng et al. (13) that activation of p38 MAPK by isoproterenol was not inhibited by carboxyl terminal region of β-AR kinase 1 (βARK-ct) in adult cardiac myocytes, suggesting that β-adrenergic p38-MAPK activation is mediated by β-arrestin–independent mechanisms. Thus, it is expected that inhibition of G protein–coupled receptor kinase (GRK) may not be sufficient to inhibit cardiomyopathy by β_2-AR overexpression, whereas addition of GRK inhibition might help suppression of cardiomyopathy by β_1-AR by eliminating the remaining components of cell signaling mediated by β-arrestin.

Although it has been recognized for some time that β_1-AR stimulation mediates apoptosis, it has been suggested that β_2-AR stimulation does not induce apoptosis (14, 16, 17) and might even protect against apoptosis (16). Stimulation of p38α MAPK has been proposed to mediate this protection (22), even though it has also been shown that β_2-AR stimulation induces protein kinase A–mediated upregulation of p38α MAPK (13), which is well known to induce apoptosis (25). Most of these studies were conducted in vitro using cell culture techniques (14, 17). Clearly, the present in vivo results in mice with β_2-AR overexpression do not support the point of view previously published (14, 16, 17). Indeed, the extent of apoptosis was similar in mice overexpressing β_2-AR and β_1-AR. Furthermore, p38α MAPK inhibition, rather than stimulation (22), was protective against development of apoptosis in the current investigation, which was conducted in vivo in mice with chronic (11–14 months) stimulation of β-AR. To reconcile these differences we examined $G_{i\alpha}$ in old β_2-AR Tg mice and found that it was significantly decreased. This result is diametrically opposite what was previously observed in vitro with administration of β_2-AR mimetic agents (14, 28). Thus, the increased $G_{i\alpha}$ observed in vitro with acute stimulation β_2-AR is protective (14, 28), but this mechanism is not invoked in the mice with chronic overexpression of β_2-AR.

Both β_1-AR Tg and β_2-AR Tg mice exhibited equivalent increases in LV hypertrophy, as reflected by the LV wt/TL ratio and by direct measurements of myocyte cross-sectional area. Interestingly, whereas the reduced LVEF was completely reversed in the bigenic β_2-AR Tg × DNp38α MAPK mice and the extent of fibrosis and apoptosis was reduced by 50%, there was no reduction in LV myocyte cross-sectional area or LV wt/TL ratio in either bigenic group. Thus, p38α MAPK appears to have an important role in mediating apoptosis (26, 29, 30), and we observed that its inhibition significantly diminished the apoptosis in bigenic β_2-AR Tg × DNp38α MAPK mice, which could be important in rescuing cardiomyopathy. However, inhibition of p38α MAPK did not affect the development of myocyte hypertrophy. Sabri et al. observed that β-AR activation of p38 MAPK alone was not sufficient to induce cardiomyocyte hypertrophy (31), which supports our results and suggests that myocyte hypertrophy is mediated by other MAPK signaling pathways. Indeed, our results in DNp38α MAPK mice demonstrated a modest increase in myocyte cross-sectional area with age, which could only partly account for the failure of DNp38α MAPK to reduce the hypertrophy in bigenic mice. Thus, inhibition, rather than stimulation, of the p38α MAPK signal induces LV hypertrophy. The study by Braz et al. also indicated that reduced p38 MAPK signaling in the heart promotes hypertrophy, potentially through calcineurin-NFAT signaling (32). It is therefore likely that the bigenic mice did not demonstrate diminution of LV hypertrophy. In contrast, a recent in vitro study concluded that p38 MAPK activity is essential for β-AR stimulation of myocyte hypertrophy (11). It has also been thought, based on in vitro studies, that β_2-AR stimulation does not induce myocyte hypertrophy (18, 19). As noted above, we observed equivalent levels of myocyte hypertrophy in mice with overexpression of cardiac β_1-AR and β_2-AR, another major difference between in vitro and in vivo results.

The results of this investigation have demonstrated several concepts that we believe to be novel. First, both mouse models of chronic β_2-AR and β_1-AR overexpression demonstrated enhanced LV function as young adults but developed equivalent severity of cardiomyopathy — in terms of reduced LVEF and increased apoptosis, fibrosis, and myocyte hypertrophy — at a similar age. Second, p38α MAPK activity was augmented significantly in both β_1-AR Tg and β_2-AR Tg models of cardiomyopathy. Third, inhibition of the p38α MAPK pathway by the *DNp38α MAPK* gene rescued the depressed LV function completely and diminished apoptosis and fibrosis in the β_2-AR Tg mice, but did not affect any of these measurements in β_1-AR Tg mice. This suggests that p38α MAPK is involved in mediating the apoptosis, fibrosis, and cardiomyopathy in β_2-AR Tg mice. In contrast, despite elevated levels of p38α MAPK activity, inhibition of p38α MAPK did not appear to prevent apoptosis and fibrosis or development of cardiomyopathy in response to chronic β_1-AR stimulation, which is likely to be mediated by other kinases, such as Mst-1. Finally, myocyte hypertrophy was not reduced by the *DNp38α MAPK* gene in either bigenic model, suggesting a clear demarcation of the effects of p38α MAPK in mediating LV hypertrophy compared with its effects on apoptosis, fibrosis, and cardiomyopathy.

The clinical relevance of the current investigation extends to other disease states that may involve β-AR signaling, including

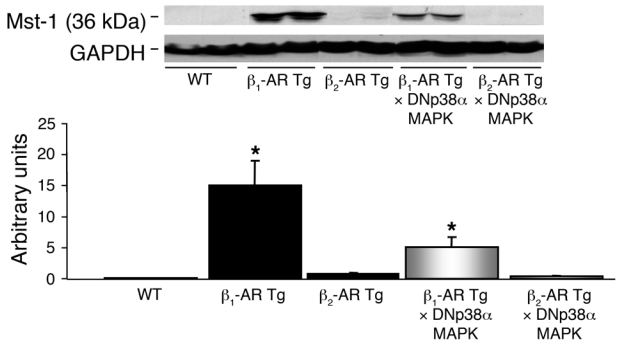

Figure 8
Cleaved Mst-1 (36 kDa) was elevated significantly in old β_1-AR Tg mice, but not old β_2-AR Tg mice, compared with age-matched WT mice. Furthermore, it remained elevated in bigenic β_1-AR Tg × DNp38α MAPK mice. *$P < 0.05$ versus WT.

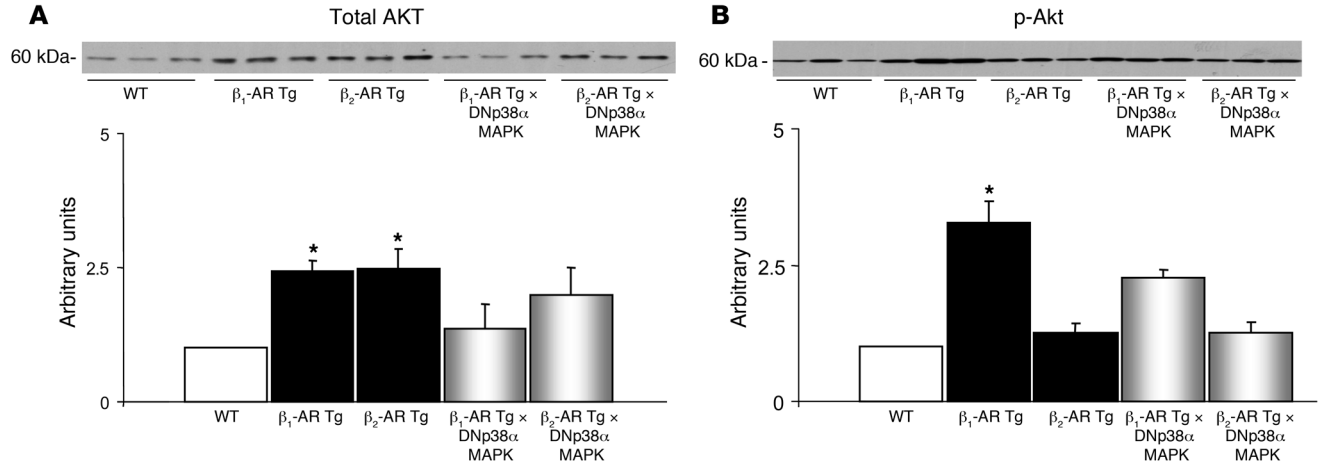

Figure 9
Akt. (**A**) Total Akt levels were elevated significantly in β_1-AR and β_2-AR Tg mice. (**B**) The level of p-Akt was significantly higher only in β_1-AR Tg mice. $n = 4$ mice per group. $^*P < 0.05$ versus WT.

asthma, hypertension, autoimmune diseases such as chronic rheumatic diseases, certain disorders of the central nervous system, and inflammatory diseases like interstitial cystitis. Most importantly, the results of the current investigation relate to the pathogenesis of HF, which is thought to involve chronically enhanced β-AR signaling (33, 34), and the treatment of HF, which now includes β-AR–blocking drugs (35–37). We speculate that distal β-AR signaling, at the level of stress-activated MAPK in general and p38α MAPK in particular, may be involved in the pathogenesis of HF. Conversely, based on the results of the current investigation and prior studies demonstrating that chronic β-AR blockade ameliorates cardiomyopathy in mice with overexpressed cardiac $G_{s\alpha}$ (38) and prevents upregulation of p38α MAPK (12), we speculate that inhibition of MAPKs may also be involved in the mechanism mediating in the beneficial effects of β-AR blockade therapy in HF, as has been shown for PKA hyperphosphorylation of the calcium release channel/cardiac ryanodine receptor (9, 10). Accordingly, inhibition of stress-activated kinases could provide a new approach to the treatment of HF.

Methods

Animals. The development and characterization of mice with cardiac-specific overexpression of β_1-AR and β_2-AR used in this study have been described previously (3, 7). Parent β_1-AR mice were obtained from the University of Wuerzburg, and parent β_2-AR mice were obtained from The Jackson Laboratory. Mice with overexpression of β_1-AR and β_2-AR were mated with mice with cardiac-specific expression of DNp38α MAPK (Taconic). In all experiments, age-matched WT littermate controls were used. All animal care and protocols were reviewed and approved by the Institutional Animal Care and Use Committee of the University of Medicine and Dentistry of New Jersey, New Jersey Medical School, Newark, New Jersey, USA.

Echocardiography. Transthoracic echocardiography was performed in young (4–6 months) and old (11–15 months) age-matched mice using an Acuson Sequoia 256 ultrasound system with a 13-MHz transducer. Mice were anesthetized with 2.5% avertin injected intraperitoneally and placed on a warmed saline bag. Electrocardiographic leads were attached to each limb using needle electrodes (Grass Technologies). After a short-axis 2-dimensional image of the LV was obtained at the level of the papillary muscles, a 2-dimensional guided M-mode trace crossing the anterior and posterior walls was recorded at a sweep speed of 200 mm/s. The following parameters were measured on the M-mode tracings using the leading-edge technique: LV internal dimensions of diastole and systole, LV external dimensions of diastole and systole, and wall thickness at diastole and systole. End-diastolic measurements were taken at the time of the apparent maximal LV diastolic dimension. End-systolic measurements were taken at the time of the most anterior systolic excursion of the posterior wall. LVEF was calculated by the cubed method as $(d^3 - s^3)/d^3$, where d and s represent LV internal dimensions of diastole and systole, respectively. Measurements were taken from 3 cardiac cycles and the mean was determined.

Western blot analysis. Protein extracts were prepared from the LVs of hearts using extraction buffer (20 mM Tris-HCl, pH 7.4, 150 mM NaCl, 1 mM EDTA, 1 mM EGTA, 1% Triton, 1 mM sodium orthovanadate, 2.5 mM sodium pyrophosphate, 1 mM β-glycerophosphate, and 5 μg/ml protease inhibitor cocktail). Protein concentration of the samples was measured with the BCA reagent from Pierce Biotechnology. Proteins were separated by SDS-PAGE, transferred to nitrocellulose membrane, and detected with specific antibodies. Blots were incubated with horseradish peroxidase–labeled secondary antibodies (goat anti-rabbit IgG). Immunoreactive bands were detected with ECL (PerkinElmer). The bands were scanned utilizing a GS800-calibrated densitometer and quantified by Quantity One software (version 4.5; Bio-Rad), and density was reported in arbitrary units. Primary antibodies used included $G_{s\alpha}$, $G_{i\alpha}$, Mst-1, p-Akt and Akt, p-MAPKAPK2 and MAPKAPK2, p-p38 MAPK and p38 MAPK, p-ERK and ERK, and p-JNK and JNK (Cell Signaling Technology). Coomassie blue staining or GAPDH antibody Western blotting was used to verify equal protein loading of the blots.

Histology. Histological studies were conducted in hearts briefly immersed in a saline wash followed by immersion in 10% buffered formalin. The heart was dissected to remove the atria and RV free wall, and each portion was weighed. Fixed tissues were dehydrated, embedded in paraffin, sectioned at 6-μm thickness, and stained with H&E. Myocardial tissue was quantitatively analyzed on a cross-section of LV obtained mid-distance from base to apex and stained with picric acid sirius red. Images were obtained from a Sony charge-coupled device video camera attached to a Nikon E800 microscope with a 10× objective and were analyzed with Image-Pro Plus image analysis software (version 5.1; New York/New Jersey Scientific Inc.). Percent collagen volume was expressed as the mean of all fields examined for each animal.

Myocyte cross-sectional area. Mean LV myocyte cross-sectional area was determined on sections stained with wheat germ agglutinin labeled with tetramethylrhodamine. Sections were taken from hearts of WT, β_1-AR Tg, bigenic β_1-AR Tg × DNp38α MAPK, β_2-AR Tg, and bigenic β_2-AR Tg × DNp38α MAPK mice. Digitized images were obtained, and the cross-sectional area was determined using Image-Pro Plus software (version 5.1; New York/New Jersey Scientific Inc.). Only cross-sectional areas in the inner third (subendocardial) and outer third (subepicardial) of the myocardium, in which capillaries were perpendicular to the section, were used to calculate the mean ± SEM for each section of myocardium.

Apoptosis. DNA fragmentation was detected in situ by using TUNEL on paraffin sections of the hearts of WT, β_1-AR Tg, β_1-AR Tg × DNp38α MAPK, β_2-AR Tg, and β_2-AR Tg × DNp38α MAPK mice. This technique has been described previously (39). Briefly, deparaffinized sections were incubated with proteinase K, and DNA fragments were labeled with biotin-conjugated deoxy UTP and terminal deoxynucleotidyl transferase and then visualized with FITC-ExtrAvidin (Sigma-Aldrich).

Statistics. Data reported are mean ± SEM. Statistical significance was evaluated using ANOVA post-hoc test. A P value less than 0.05 was considered significant.

Acknowledgments

This work was supported by NIH grants HL59139, HL69020, AG23137, AG14121, HL65183, HL65182, HL69752, HL33107, HL67724, AG23039, and GM67773.

Received for publication July 5, 2006, and accepted in revised form February 13, 2007.

Address correspondence to: Dorothy E. Vatner, New Jersey Medical School, University of Medicine and Dentistry of New Jersey, 185 South Orange Avenue, MSB G609, Newark, New Jersey 07103, USA. Phone: (973) 972-8920; Fax: (973) 972-7489; E-mail: vatnerdo@umdnj.edu.

1. Bristow, M.R. 2000. β-adrenergic receptor blockade in chronic heart failure. *Circulation.* **101**:558–569.
2. Du, X.J., et al. 2000. Age-dependent cardiomyopathy and heart failure phenotype in mice overexpressing beta(2)-adrenergic receptors in the heart. *Cardiovasc. Res.* **48**:448–454.
3. Engelhardt, S., Hein, L., Wiesmann, F., and Lohse, M.J. 1999. Progressive hypertrophy and heart failure in beta1-adrenergic receptor transgenic mice. *Proc. Natl. Acad. Sci. U. S. A.* **96**:7059–7064.
4. Felker, G.M., and O'Connor, C.M. 2001. Inotropic therapy for heart failure: an evidence-based approach. *Am. Heart J.* **142**:393–401.
5. Iwase, M., et al. 1996. Adverse effects of chronic endogenous sympathetic drive induced by cardiac GS alpha overexpression. *Circ. Res.* **78**:517–524.
6. Liggett, S.B., et al. 2000. Early and delayed consequences of beta(2)-adrenergic receptor overexpression in mouse hearts: critical role for expression level. *Circulation.* **101**:1707–1714.
7. Milano, C.A., et al. 1994. Enhanced myocardial function in transgenic mice overexpressing the beta 2-adrenergic receptor. *Science.* **264**:582–586.
8. Vatner, S.F., Vatner, D.E., and Homcy, C.J. 2000. Beta-adrenergic receptor signaling: an acute compensatory adjustment-inappropriate for the chronic stress of heart failure? Insights from Gsalpha overexpression and other genetically engineered animal models. *Circ. Res.* **86**:502–506.
9. Reiken, S., et al. 2003. Beta-blockers restore calcium release channel function and improve cardiac muscle performance in human heart failure. *Circulation.* **107**:2459–2466.
10. Wehrens, X.H., and Marks, A.R. 2004. Novel therapeutic approaches for heart failure by normalizing calcium cycling. *Nat. Rev. Drug Discov.* **3**:565–573.
11. Wenzel, S., Muller, C., Piper, H.M., and Schluter, K.D. 2005. p38 MAP-kinase in cultured adult rat ventricular cardiomyocytes: expression and involvement in hypertrophic signalling. *Eur. J. Heart Fail.* **7**:453–460.
12. Karoor, V., et al. 2004. Propranolol prevents enhanced stress signaling in Gs alpha cardiomyopathy: potential mechanism for beta-blockade in heart failure. *J. Mol. Cell. Cardiol.* **36**:305–312.
13. Zheng, M., et al. 2000. Beta 2-adrenergic receptor-induced p38 MAPK activation is mediated by protein kinase A rather than by Gi or gbeta gamma in adult mouse cardiomyocytes. *J. Biol. Chem.* **275**:40635–40640.
14. Zheng, M., Zhu, W., Han, Q., and Xiao, R.P. 2005. Emerging concepts and therapeutic implications of beta-adrenergic receptor subtype signaling. *Pharmacol. Ther.* **108**:257–268.
15. Xiao, R.P., et al. 2003. Enhanced G(i) signaling selectively negates beta2-adrenergic receptor (AR)–but not beta1-AR-mediated positive inotropic effect in myocytes from failing rat hearts. *Circulation.* **108**:1633–1639.
16. Xiao, R.P., et al. 2004. Subtype-specific beta-adrenoceptor signaling pathways in the heart and their potential clinical implications. *Trends Pharmacol. Sci.* **25**:358–365.
17. Zhu, W.Z., et al. 2003. Linkage of β_1-adrenergic stimulation to apoptotic heart cell death through protein kinase A–independent activation of Ca^{2+}/calmodulin kinase II. *J. Clin. Invest.* **111**:617–625. doi:10.1172/JCI200316326.
18. Morisco, C., Zebrowski, D.C., Vatner, D.E., Vatner, S.F., and Sadoshima, J. 2001. Beta-adrenergic cardiac hypertrophy is mediated primarily by the beta(1)-subtype in the rat heart. *J. Mol. Cell. Cardiol.* **33**:561–573.
19. Schafer, M., Frischkopf, K., Taimor, G., Piper, H.M., and Schluter, K.D. 2000. Hypertrophic effect of selective beta(1)-adrenoceptor stimulation on ventricular cardiomyocytes from adult rat. *Am. J. Physiol. Cell Physiol.* **279**:C495–C503.
20. Zhang, S., et al. 2003. The role of the Grb2–p38 MAPK signaling pathway in cardiac hypertrophy and fibrosis. *J. Clin. Invest.* **111**:833–841. doi:10.1172/JCI200316290.
21. Yamamoto, S., et al. 2003. Activation of Mst1 causes dilated cardiomyopathy by stimulating apoptosis without compensatory ventricular myocyte hypertrophy. *J. Clin. Invest.* **111**:1463–1474. doi:10.1172/JCI200317459.
22. Communal, C., Colucci, W.S., and Singh, K. 2000. p38 mitogen-activated protein kinase pathway protects adult rat ventricular myocytes against beta-adrenergic receptor-stimulated apoptosis. Evidence for Gi-dependent activation. *J. Biol. Chem.* **275**:19395–19400.
23. Communal, C., Singh, K., Sawyer, D.B., and Colucci, W.S. 1999. Opposing effects of beta(1)- and beta(2)-adrenergic receptors on cardiac myocyte apoptosis: role of a pertussis toxin-sensitive G protein. *Circulation.* **100**:2210–2212.
24. Adams, J.W., et al. 1998. Enhanced Galphaq signaling: a common pathway mediates cardiac hypertrophy and apoptotic heart failure. *Proc. Natl. Acad. Sci. U. S. A.* **95**:10140–10145.
25. Baines, C.P., and Molkentin, J.D. 2005. STRESS signaling pathways that modulate cardiac myocyte apoptosis. *J. Mol. Cell. Cardiol.* **38**:47–62.
26. Wang, Y., et al. 1998. Cardiac muscle cell hypertrophy and apoptosis induced by distinct members of the p38 mitogen-activated protein kinase family. *J. Biol. Chem.* **273**:2161–2168.
27. Liao, P., et al. 2001. The in vivo role of p38 MAP kinases in cardiac remodeling and restrictive cardiomyopathy. *Proc. Natl. Acad. Sci. U. S. A.* **98**:12283–12288.
28. Xiao, R.P., Ji, X., and Lakatta, E.G. 1995. Functional coupling of the beta 2-adrenoceptor to a pertussis toxin-sensitive G protein in cardiac myocytes. *Mol. Pharmacol.* **47**:322–329.
29. Engelbrecht, A.M., Niesler, C., Page, C., and Lochner, A. 2004. p38 and JNK have distinct regulatory functions on the development of apoptosis during simulated ischaemia and reperfusion in neonatal cardiomyocytes. *Basic Res. Cardiol.* **99**:338–350.
30. Ren, J., Zhang, S., Kovacs, A., Wang, Y., and Muslin, A.J. 2005. Role of p38alpha MAPK in cardiac apoptosis and remodeling after myocardial infarction. *J. Mol. Cell. Cardiol.* **38**:617–623.
31. Sabri, A., Pak, E., Alcott, S.A., Wilson, B.A., and Steinberg, S.F. 2000. Coupling function of endogenous alpha(1)- and beta-adrenergic receptors in mouse cardiomyocytes. *Circ. Res.* **86**:1047–1053.
32. Braz, J.C., et al. 2003. Targeted inhibition of p38 MAPK promotes hypertrophic cardiomyopathy through upregulation of calcineurin-NFAT signaling. *J. Clin. Invest.* **111**:1475–1486. doi:10.1172/JCI200317295.
33. Bristow, M.R., et al. 1986. Beta 1- and beta 2-adrenergic-receptor subpopulations in nonfailing and failing human ventricular myocardium: coupling of both receptor subtypes to muscle contraction and selective beta 1-receptor down-regulation in heart failure. *Circ. Res.* **59**:297–309.
34. Steinberg, S.F. 1999. The molecular basis for distinct beta-adrenergic receptor subtype actions in cardiomyocytes. *Circ. Res.* **85**:1101–1111.
35. Foody, J.M., Farrell, M.H., and Krumholz, H.M. 2002. Beta-blocker therapy in heart failure: scientific review. *JAMA.* **287**:883–889.
36. Swedberg, K., Hjalmarson, A., Waagstein, F., and Wallentin, I. 1979. Prolongation of survival in congestive cardiomyopathy by beta-receptor blockade. *Lancet.* **1**:1374–1376.
37. Packer, M. 1998. Beta-adrenergic blockade in chronic heart failure: principles, progress, and practice. *Prog. Cardiovasc. Dis.* **41**:39–52.
38. Asai, K., et al. 1999. β-Adrenergic receptor blockade arrests myocyte damage and preserves cardiac function in the transgenic $G_{s\alpha}$ mouse. *J. Clin. Invest.* **104**:551–558.
39. Okumura, S., et al. 2003. Disruption of type 5 adenylyl cyclase gene preserves cardiac function against pressure overload. *Proc. Natl. Acad. Sci. U. S. A.* **100**:9986–9990.